MATEMATIKA, 2008, Volume 24, Number 2, 187–198


# The Unsteady Power Law Blood Flow Through a Multi-irregular Stenosed Artery

[1]**Norzieha Mustapha &** [2]**Norsarahaida Amin**
Department of Mathematics, Faculty of Science, Universiti Teknologi Malaysia,
81310 UTM Skudai, Johor, Malaysia.
e-mail: [1]norzieha@mel.fs.utm.my, [2]norsarahaida@utm.my

**Abstract** A non-Newtonian pulsatile model of blood flow through multiple stenoses with irregular surfaces is considered. The model chosen is the generalized power law model of blood viscocity where the flow is assumed to be unsteady, laminar, two-dimensional and axisymmetric. The governing equations of motion in terms of the viscous shear stress and the boundary conditions in the cylindrical coordinate system are first transformed using a radial coordinate transformation before they are discretized using a finite difference scheme based on central difference approximations on non-uniform grids. The numerical results obtained in terms of blood flow characterictics show that the values of the axial velocity and flow rate in the power-law model are lower while the resistance to flow and the wall shear stress are higher compared to the Newtonian model. These features concur with the general observations of blood flowing through small stenosed arteries.

**Keywords** Power-law; multi-irregular; stenosed artery; blood flow; non-Newtonian.

## 1 Introduction

The cause and development of cardiovascular diseases are related to the nature of blood movement and the mechanical behaviour of the blood vessel walls. The rheological behaviour of blood can be characterized by a non-Newtonian viscosity and may depend on the vessel size. In the case of blood flowing in a large artery whose radius is larger than 1 mm, the blood behaviour can be assumed as Newtonian. However, this assumption is not valid when the blood vessel is smaller i.e having a radius less than 1mm. See Mandal [1].

From a biofluid mechanics point of view, blood would not be expected to obey the very simple, one parameter, and linearised law of viscosity developed by Newton. As mentioned by Enderle et al. [2]), the non-Newtonian characteristics of blood can only be modelled by higher order constitutive equations. Significant attempts to define such non-Newtonian behaviour, however did not appear until the 1960s, when variable-shear rotational viscometers were introduced. Since then, literally dozens of constitutive models that attempted to relate shear stress to shear rate in the fluid have been proposed. The most practical of these is an empirical power law formulation that generalizes Newton's law of viscocity.

Charm and Kurland [3] observed that the shear rate versus apparent blood viscosity data of canine blood followed those of power law fluids. Experimental findings of Perktold

et al. [4] showed that the power law fluid exhibits a non-Newtonian influence. Hussain et al. [5] noted that all blood samples of 259 patients in their study behave as a non-Newtonian power law fluid. Tu and Deville [6] , pointed out that the blood of patients in some disease conditions, for example patients with severe myocardial infarction, cerebrovascular diseases and hypertension, exhibits power law properties.

The above studies considered blood flow through a single stenosis. However, in many clinical situations, the patient is found to have multiple stenoses, i.e., more than one stenosis in the same arterial segment (Talukder et al. [7]). (Fukushima et al. [8]) and Johnston and Kilpatrick [9] have studied Newtonian blood flow through a pair of multiple stenoses while (Ang and Mazumdar [10]) considered triplet stenoses. Their studies showed that multiple stenoses have more significant effects on blood flow compared to the sum of the effects of the individual stenoses.

In most of the studies mentioned above, the geometry of stenosis was represented by a cosine curve in contrast to the real situation where the geometry of stenosis is more likely to be irregular. (Johnston and Kilpatrick [11], Anderson et al. [12], Chakravarty et al. [13], and Yakhot et al. [14]) observed that an artery modelled by a smooth curve of the same severity overestimated the pressure drop, wall shear stress and the separation Reynolds number compared to an artery modelled by an irregular curve.

In view of the above findings and in an effort to resemble the in vivo situation, the present work considers the power law model of blood flow through a multi-irregular stenosed artery. The governing equations, boundary conditions and the geometry of stenosis considered are presented in sections 2 and 3 while the solution procedure is described in sections 4 and 5. The numerical results which compare the blood flow characteristics of the power-law model with the Newtonian model is discussed in section 6.

## 2 Governing equations

Consider the case of power law fluid representing stenotic blood flowing through a straight arterial vessel, rigid and axisymmetric with the present of a multi-irregular stenoses. The flow is laminar, unsteady, two-dimensional, and fully developed where the flowing blood is treated to be an incompressible fluid. Under these assumptions, the governing equations may be written in the cylindrical coordinates system as:

Equation of axial momentum

$$\frac{\partial w}{\partial t} + w\frac{\partial w}{\partial r} + u\frac{\partial w}{\partial z} = -\frac{1}{\rho}\frac{\partial p}{\partial z} - \frac{1}{\rho}\left[\frac{1}{r}\frac{\partial}{\partial r}\left(r\tau_{rz}\right) + \frac{\partial}{\partial z}\left(\tau_{zz}\right)\right], \tag{1}$$

equation of radial momentum

$$\frac{\partial u}{\partial t} + u\frac{\partial u}{\partial r} + w\frac{\partial u}{\partial z} = -\frac{1}{\rho}\frac{\partial p}{\partial r} - \frac{1}{\rho}\left[\frac{1}{r}\frac{\partial}{\partial r}\left(r\tau_{rr}\right) + \frac{\partial}{\partial z}\left(\tau_{rz}\right)\right] \tag{2}$$

and equation of continuity

$$\frac{\partial u}{\partial r} + \frac{u}{r} + \frac{\partial w}{\partial z} = 0, \tag{3}$$

where the relationship between the shear stress and the shear rate in case of two dimensional

motions are (see Bird et al. [15]):

$$\tau_{zz} = -2\left\{ m \left| \left[ \left(\frac{\partial u}{\partial r}\right)^2 + \left(\frac{u}{r}\right)^2 + \left(\frac{\partial w}{\partial z}\right)^2 + \left(\frac{\partial u}{\partial z} + \frac{\partial w}{\partial r}\right)^2 \right]^{\frac{1}{2}} \right|^{n-1} \right\} \left(\frac{\partial w}{\partial z}\right), \tag{4}$$

$$\tau_{rz} = -\left\{ m \left| \left[ \left(\frac{\partial u}{\partial r}\right)^2 + \left(\frac{u}{r}\right)^2 + \left(\frac{\partial w}{\partial z}\right)^2 + \left(\frac{\partial u}{\partial z} + \frac{\partial w}{\partial r}\right)^2 \right]^{\frac{1}{2}} \right|^{n-1} \right\} \left(\frac{\partial w}{\partial r} + \frac{\partial u}{\partial z}\right) \tag{5}$$

and

$$\tau_{rr} = -2\left\{ m \left| \left[ \left(\frac{\partial u}{\partial r}\right)^2 + \left(\frac{u}{r}\right)^2 + \left(\frac{\partial w}{\partial z}\right)^2 + \left(\frac{\partial u}{\partial z} + \frac{\partial w}{\partial r}\right)^2 \right]^{\frac{1}{2}} \right|^{n-1} \right\} \left(\frac{\partial u}{\partial r}\right). \tag{6}$$

Here $\tau$ is the stress tensor and $n$ is the fluid behaviour index parameter. Following Pedley [16], under certain assumptions, the axial viscous transport terms are negligible and the radial equation of motion simply reduces to $\partial p/\partial r = 0$, indicating that the pressure is independent of radial position. Hence, equation (2) can be omitted. Following Burton [17], for a human being, the pressure gradient $\partial p/\partial z$ appearing in (1) is taken as

$$-\frac{\partial p}{\partial z} = A_0 + A_1 \cos(\omega t) \tag{7}$$

where $A_0$ is the constant amplitude of the pressure gradient, $A_1$ is the amplitude of the pulsatile component giving rise to systolic and diastolic pressure; $\omega = 2\pi f_p$, where $f_p$ is the pulse frequency.

The boundary conditions on the solid wall are the no slip conditions:

$$w(r, z, t) = 0, \quad u(r, z, t) = 0 \text{ at } r = R. \tag{8}$$

and in the tube, the condition is

$$\frac{\partial w(r, z, t)}{\partial r} = 0, \quad u(r, z, t) = 0 \text{ at } r = 0. \tag{9}$$

For a system at rest;

$$w(r, z, t) = 0 \text{ and } u(r, z, t) = 0 \text{ at } t = 0. \tag{10}$$

## 3 Geometry of Stenoses

The geometry of stenosis considered here is the rough or irregular profile, which is constructed from the data developed by Back et al. [18]. The profile of multiple stenoses with irregular and smooth geometry represented by cosine curves are shown in Figure 1. The irregular shape of the first and second artery is assumed to be the same.

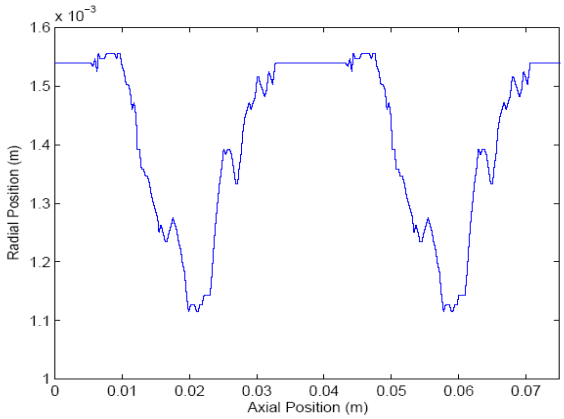


Figure 1: Profile of Multiple Irregular Stenoses

## 4 Transformation of the Governing Equations

### 4.1 Radial Coordinate Transformation

Using a radial coordinate transformation $x = \frac{r}{R(z)}$ , which has the effect of immobilizing the vessel wall in the transformed coordinate $x$, the continuity equation (3) and the equation of motion (1) , the relationship between the shear stress and shear rate, (4) and (5) become:

$$\frac{1}{R}\frac{\partial u}{\partial x} + \frac{u}{xR} + \frac{\partial w}{\partial z} - \frac{x}{R}\frac{\partial w}{\partial x}\frac{\partial R}{\partial z} = 0, \tag{11}$$

$$\begin{aligned}\frac{\partial w}{\partial t} = &\left[\frac{x}{R}\frac{\partial R}{\partial t} - \frac{u}{R} + w\frac{x}{R}\frac{\partial R}{\partial z}\right]\frac{\partial w}{\partial x} \\ &- w\frac{\partial w}{\partial z} - \frac{1}{\rho}\frac{\partial p}{\partial z} - \frac{1}{\rho}\left[\frac{1}{xR}\tau_{xz} + \frac{1}{R}\frac{\partial \tau_{xz}}{\partial x} + \frac{\partial \tau_{zz}}{\partial z} - \frac{x}{R}\frac{\partial \tau_{xz}}{\partial x}\frac{\partial R}{\partial z}\right],\end{aligned} \tag{12}$$

with

$$\begin{aligned}\tau_{zz} = -2\Bigg\{m\Bigg|\Bigg[&\left(\frac{1}{R}\frac{\partial u}{\partial x}\right)^2 + \left(\frac{u}{xR}\right)^2 + \left(\frac{\partial w}{\partial z} - \frac{x}{R}\frac{\partial R}{\partial z}\frac{\partial w}{\partial x}\right)^2 \\ &+ \left(\frac{\partial u}{\partial z} - \frac{x}{R}\frac{\partial R}{\partial z}\frac{\partial u}{\partial x} + \frac{1}{R}\frac{\partial w}{\partial x}\right)^2\Bigg]^{\frac{1}{2}}\Bigg|^{n-1}\Bigg\}\left(\frac{\partial w}{\partial z} - \frac{x}{R}\frac{\partial R}{\partial z}\frac{\partial w}{\partial x}\right),\end{aligned} \tag{13}$$

$$\begin{aligned}\tau_{xz} = -\Bigg\{m\Bigg|\Bigg[&\left(\frac{1}{R}\cdot\frac{\partial u}{\partial x}\right)^2 + \left(\frac{u}{xR}\right)^2 + \left(\frac{\partial w}{\partial z} - \frac{x}{R}\frac{\partial R}{\partial z}\frac{\partial w}{\partial x}\right)^2 \\ &+ \left(\frac{\partial u}{\partial z} - \frac{x}{R}\frac{\partial R}{\partial z}\frac{\partial u}{\partial x} + \frac{1}{R}\frac{\partial w}{\partial x}\right)^2\Bigg]^{\frac{1}{2}}\Bigg|^{n-1}\Bigg\}\left(\frac{1}{R}\frac{\partial w}{\partial x} + \frac{\partial u}{\partial z} - \frac{x}{R}\frac{\partial R}{\partial z}\frac{\partial u}{\partial x}\right).\end{aligned} \tag{14}$$

The boundary and initial conditions (8) – (10) now become:

$$\left.\begin{array}{l} u\,(x,z,t)=0,\ w\,(x,z,t)=0\ \text{on}\ x=1, \\ u\,(x,z,t)=0,\ \dfrac{\partial\, w\ (x,z,t)}{\partial\, x}=0,\ \tau_{\mathrm{rz}}=0\ \text{on}\ x=0 \\ \text{and}\ u\,(x,z,t)=0=w\,(x,z,t)\ \text{at}\ t=0. \end{array}\right\} \tag{15}$$

### 4.2 The Radial Momentum

In order to obtain an expression for the radial velocity component, $u\ (x,z,t)$ equation (11) is multiplied by $xR$ and integrated with respect to $x$, to obtain ,

$$\int x\frac{\partial\, w}{\partial\, x}\,dx+\int\ w\ dx+\int\ xR\frac{\partial\, u}{\partial\, z}\,dx-\int\ x^2\frac{\partial w}{\partial\, x}\cdot\frac{\partial\, R}{\partial\, z}\,dx=0 \tag{16}$$

Simplification of the above equation gives

$$xw+R\int\ x\frac{\partial\, u}{\partial\, z}\,dx-\frac{\partial\, R}{\partial\, z}x^2u+\frac{\partial\, R}{\partial\, z}\int\ 2xu\ dx=0 \tag{17}$$

which upon arranging gives

$$u=x\frac{\partial\, R}{\partial\, z}w-\frac{R}{x}\int\ x\frac{\partial\, w}{\partial\, z}\,dx-\frac{2}{x}\frac{\partial\, R}{\partial\, z}\int\ xw\ dx\quad . \tag{18}$$

Taking into account the boundary condition (15b) Equation (18) takes the following form;

$$-\int_0^1\ x\frac{\partial\, w}{\partial\, z}\,dx=\int_0^1\ x\left[\frac{2}{R}\frac{\partial\, R}{\partial\, z}w\right]\,dx \tag{19}$$

Comparing the LHS and RHS of equation (19), gives

$$\frac{\partial\, w}{\partial\, z}=-\frac{2}{R}\frac{\partial\, R}{\partial\, z}w \tag{20}$$

Then, substituting equation (20) into equation (18) and simplifying, gives

$$u(x,z,t)=x\left[\frac{\partial\, R}{\partial\, z}w\right] \tag{21}$$

Equation (21) is new sum of the radial velocity component that needs to be calculated.

## 5 Numerical Procedure

The finite difference scheme for discretizing equations (11) and (12) is based on the central difference approximations for all the first spatial derivatives in the following manner.

$$\frac{\partial w}{\partial x}=\frac{(w)^k_{i,j+1}-(w)^k_{i,j-1}}{2\Delta x_j} \tag{22}$$

$$\frac{\partial^2 w}{\partial x^2}=\frac{(w)^k_{i,j+1}-2(w)^k_{i,j}+(w)^k_{i,j-1}}{(\Delta x_j)^2} \tag{23}$$

$$\frac{\partial w}{\partial z} = \frac{(w)^k_{i+1,j}\Delta z^2_{i-1} + (w)^k_{i,j}(\Delta z^2_i - \Delta z^2_{i-1}) - (w)^k_{i-1,j}\Delta z^2_i}{\Delta z^{\Delta}_i z^{(}_{i-1}\Delta z^{+}_i \Delta z^{)}_{i-1}} \tag{24}$$

$$\frac{\partial^2 w}{\partial z^2} = 2\frac{(w)^k_{i+1,j}\Delta z_{i-1} - (w)^k_{i,j}(\Delta z_i + \Delta z_{i-1}) + (w)^k_{i-1,j}\Delta z_i}{\Delta z_i \Delta z_{i-1}(\Delta z_i + \Delta z_{i-1})}, \tag{25}$$

with the errors of $\mathrm{O}(\Delta x_j)^2$ and $\mathrm{O}(\Delta z_i)^2$. The time derivative in (12) is approximated using forward approximations to obtain the difference quotient

$$\frac{\partial w}{\partial t} = \frac{(w)^{k+1}_{i,j} - (w)^k_{i,j}}{\Delta t}.$$

with the error of $\mathrm{O}(\Delta t)^2$.

Other spatial derivatives can be obtained from similar expressions. The notation used in this section is $w(z,x,t) \equiv w(z_i, x_j, t_k) \equiv w^k_{i,j}$. Defining

$$x_j = (j-1)\Delta x,\ j = 1, 2, \ldots N+1$$

such that $x_{N+1}$=1.0, $\Delta z_i = z_{i+1} - z_i\ i = 1, 2, \ldots M$) and $t_k = (k-1)\Delta t,\ k = 1, 2, \ldots$ for the entire arterial segment under study with $\Delta x$, the increment in the radial direction and $\Delta z$ is the non-uniform increment in the axial direction.

Using equations (22) – (25), the discretized form of equations (11) – (14) are given as:

$$\begin{aligned}(w)^{k+1}_{i,j} = (w)^k_{i,j} + \Delta t \Bigg\{ & \left[ \frac{(u)^k_{i,j}}{R^k_i} + (w)^k_{i,j}\, \frac{x_j}{R^k_i} \left( \frac{\partial R}{\partial z} \right)^k_i \right] \left( \frac{\partial w}{\partial x} \right)^k_{i,j} \\ & - (w)^k_{i,j} \left( \frac{\partial w}{\partial z} \right)^k_{i,j} - \frac{1}{\rho} \left( \frac{\partial p}{\partial z} \right)^{k+1} - \frac{1}{\rho} \left[ \frac{1}{x_j R^k_i} (\tau_{xz})^k_{i,j} + \frac{1}{R^k_i} \left( \frac{\partial \tau_{xz}}{\partial x} \right)^k_{i,j} \right. \\ & \left. + \left( \frac{\partial \tau_{zz}}{\partial z} \right)^k_{i,j} - \frac{x_j}{R^k_i} \left( \frac{\partial \tau_{xz}}{\partial x} \right)^k_{i,j} \left( \frac{\partial R}{\partial z} \right)^k_i \right] \Bigg\}, \end{aligned} \tag{26}$$

$$\begin{aligned}(\tau_{zz})^k_{i,j} = -2 \Bigg\{ & m \Bigg| \Bigg[ \left( \frac{1}{R^k_i} \left( \frac{\partial u}{\partial x} \right)^k_{i,j} \right)^2 + \left( \frac{(u)^k_{i,j}}{x_j R^k_i} \right)^2 \\ & + \left( \left( \frac{\partial w}{\partial z} \right)^k_{i,j} - \frac{x_j}{R^k_i} \left( \frac{\partial R}{\partial z} \right)^k_i \left( \frac{\partial w}{\partial x} \right)^k_{i,j} \right)^2 + \left( \left( \frac{\partial u}{\partial z} \right)^k_{i,j} - \frac{x_j}{R^k_i} \left( \frac{\partial R}{\partial z} \right)^k_i \left( \frac{\partial u}{\partial x} \right)^k_{i,j} \right. \\ & \left. + \frac{1}{R^k_i} \left( \frac{\partial w}{\partial x} \right)^k_{i,j} \right)^2 \Bigg]^{\frac{1}{2}} \Bigg|^{n-1} \Bigg\} \left( \left( \frac{\partial w}{\partial z} \right)^k_{ij} - \frac{x_j}{R^k_i} \left( \frac{\partial R}{\partial z} \right)^k_i \left( \frac{\partial w}{\partial x} \right)^k_{ij} \right), \end{aligned} \tag{27}$$

$$(\tau_{xz})^k_{i,j} = -\left\{ m \left| \left[ \left( \frac{1}{R_i^k} \left( \frac{\partial u}{\partial x} \right)^k_{i,j} \right)^2 + \left( \frac{(u)^k_{i,j}}{x_j R_i^k} \right)^2 + \left( \left( \frac{\partial w}{\partial z} \right)^k_{i,j} - \frac{x_j}{R_i^k} \left( \frac{\partial R}{\partial z} \right)^k_i \left( \frac{\partial w}{\partial x} \right)^k_{i,j} \right)^2 \right.\right.$$
$$\left.\left. + \left( \left( \frac{\partial u}{\partial z} \right)^k_{i,j} - \frac{x_j}{R_i^k} \left( \frac{\partial R}{\partial z} \right)^k_i \left( \frac{\partial u}{\partial x} \right)^k_{i,j} + \frac{1}{R_i^k} \left( \frac{\partial w}{\partial x} \right)^k_{i,j} \right)^2 \right]^{\frac{1}{2}} \right|^{n-1} \right\} \left( \left( \frac{\partial u}{\partial z} \right)^k_{i,j} \right.$$
$$\left. - \frac{x_j}{R_i^k} \left( \frac{\partial R}{\partial z} \right)^k_i \left( \frac{\partial u}{\partial x} \right)^k_{i,j} + \frac{1}{R_i^k} \left( \frac{\partial w}{\partial x} \right)^k_{i,j} \right). \tag{28}$$

The discretized boundary conditions are given by

$$w^k_{i,1} = w^k_{i,2}, \quad u^k_{i,1} = 0, \quad u^k_{i,N+1} = 0, \quad w^k_{i,N+1} = 0, \quad \text{and} \quad (u)^1_{i,j} = 0, \ (w)^1_{i,j} = 0. \tag{29}$$

The axial velocity component is obtained using the equations (26) - (28), together with the boundary conditions (29). The radial velocity component from equation (21) can be rewritten in discretized form as

$$(u)^{k+1}_{i,j} = x_j \left[ \left( \frac{\partial R}{\partial z} \right)^k_i (w)^{k+1}_{i,j} \right] \tag{30}$$

The radial velocity component can be calculated directly from equation (30), using the values of the axial velocity component. The explicit finite difference scheme presented above is limited by the stability criterion

$$\Delta t \leq \frac{1}{8} \frac{(\Delta x_j)^2 + (\Delta z_i)^2}{k}. \tag{31}$$

Blood flow characteristics such as the volumetric flow rate ($Q$), the resistance to flow ($\Omega$), the wall shear stress ($\tau_w$) can be obtained from the following relations,

$$Q^k_i = 2\pi \left( R^k_i \right)^2 \int_0^1 x_j \, (w)^k_{i,j} \, dx_j \tag{32}$$

$$\Omega^k_i = \frac{\left| L \left( \partial p / \partial z \right)^k \right|}{Q^k_i} \tag{33}$$

$$(\tau_w)^k_i = (\tau_{xz})^k_{i,j} \times \cos \left[ \arctan \left( \frac{\partial R}{\partial z} \right)^k_i \right] \tag{34}$$

## 6 Numerical Results and Discussions

Numerical computations were carried out using the Gauss-Seidel algorithm with the following parameter values :

$$L = 0.1746, f_p = 1.2\text{Hz}, \rho = 1.06\text{x}10^3\text{Kgm}^{-3}, \mu = 0.0035 \text{ Pa},$$
$$\text{A}_1 = 100 \text{ Kgm}^{-2}\text{s}^{-2}, \text{A}_0 = 0.2\text{A}_1, \Delta x = 0.025, \Delta t = 0.00001.$$

The results in terms of velocity profiles, flow rate, resistance to flow and wall shear stress are compared with those obtained using the Newtonian model.

### 6.1 Velocity Profiles

Figure 2 illustrates the variation of the axial velocity profiles in an artery containing multiple stenoses for different times spread over a single cardiac cycle. The velocity presented is evaluated at the critical height of the first stenosis (when z=0.018m) at different time periods. The blood is assumed to be in the early diastole phase for a single cardiac cycle when the time reaches 0.5s, when the flow is at minimum. It can be seen that the flow velocity is reduced when the time is 0.25s to 0.5s but at time equals to 0.7s the velocity curve is found to shift away from the origin. This is due to the pulsatility of the pressure gradient produced by the heart as it comes into play. Compared to the Newtonian model, the velocity for the power law model is lower for all times periods.

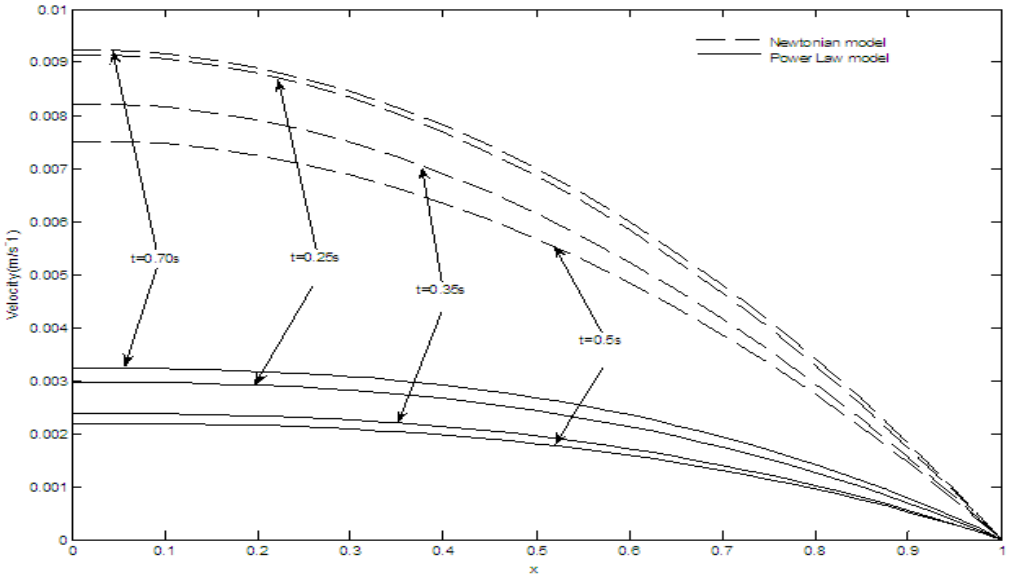


Figure 2: Axial Velocity Profiles for Blood Flow Through Multi-irregular Stenoses

### 6.2 Flow Rates and Resistance to Flow

Figures 3 and 4 exhibit how the non-Newtonian rheology of the streaming blood affects the rate of flow and the resistance to flow at different times. The flow rate for the Newtonian model of blood viscosity is higher while the resistive impedance is lower compared to the corresponding values in the power law model.

### 6.3 Wall Shear Stress

The wall shear stress is the representation of the magnitude and rate of change of blood flow close to a vessel wall and has been linked to the pathogenesis of atherosclerosis. Wall

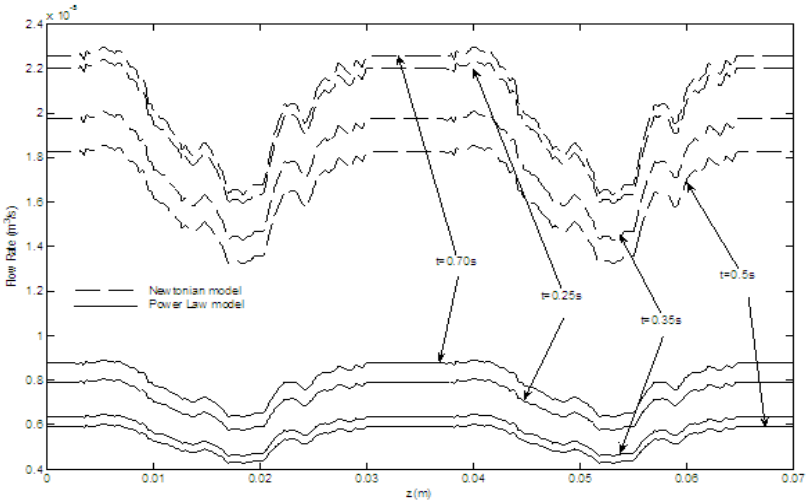


Figure 3: Flow Rates for a Multi-irregular Stenoses at Different Time Periods

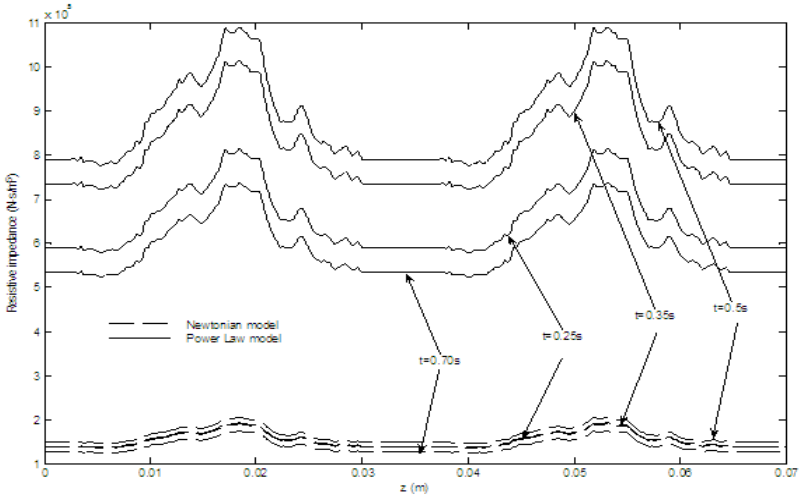


Figure 4: Resistance to Flow Rates for a Multi-irregular Stenoses at Different Time Periods

shear stress mapping should become part of the important approach to early detection of atherosclerosis. Figure 5 exhibits the behaviour of the wall shear stress distributed over the arterial segment for the four different time periods and also their responses to the blood viscosity. In the multiple irregular stenoses with 48% areal occlusion, a Newtonian model of blood viscosity predicts lower shear stress than a power law model. As time progresses, the stresses appear to decrease until the time 0.5s of a single cardiac cycle. However, the values of the wall shear stress increase when the time is 0.7s. One may point out in this regard that the stress reduces in magnitude during the systolic phase and increase at the diastolic phase of a single cardiac cycle which is when the system is activated under the normal functioning of the heart producing a pressure gradient.

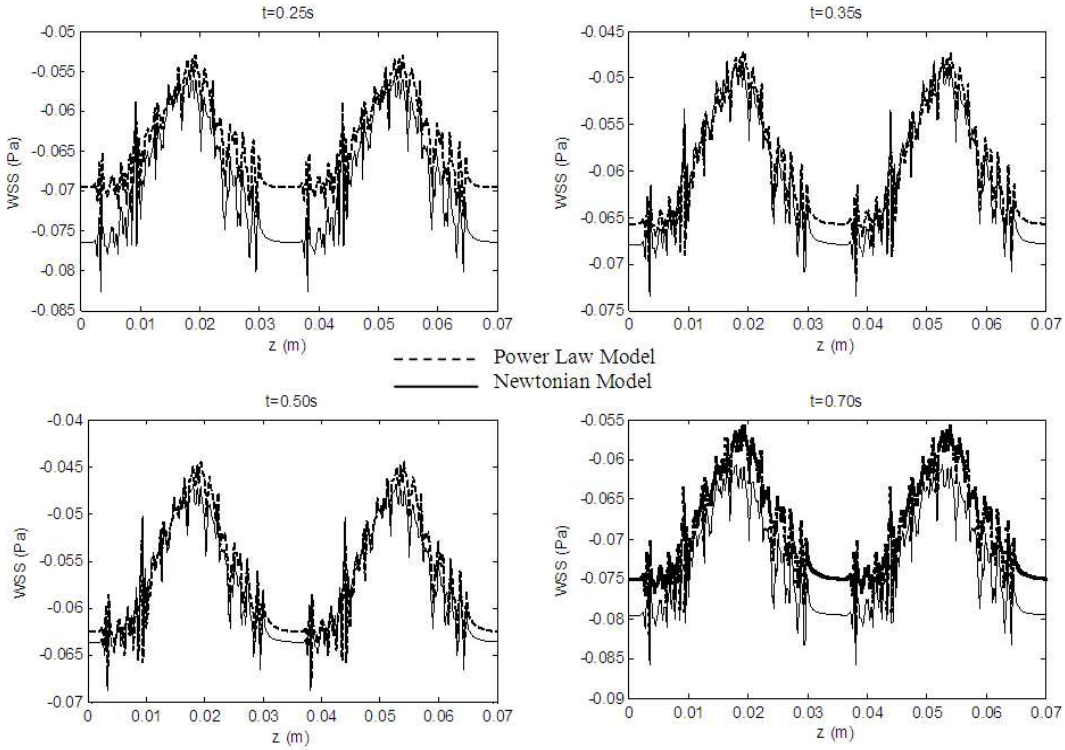


Figure 5: Wall Shear Stress for Multi-irregular Stenoses at Different Time Periods

## 7 Conclusions

Numerical results for an unsteady blood flow in a multi-irregular stenosed artery, using the power law model of blood viscosity have been presented. Comparison of the blood flow characteristics with the results from the Newtonian model show that the axial velocities and flow rates are lower while the resistance to flow and the wall shear stress values are higher in the case of power-law model. These results confirm earlier experimental observations that

blood flow through small arteries exhibit non-Newtonian behavior.

## 8 Acknowledgments

Financial support provided by JPA (SLAB),UTM and FRGS Vot 78087 is gratefully acknowledged.

## References

[1] P.K. Mandal, *An Unsteady Analysis of Non-Newtonian Blood Flow through Tapered Arteries with a Stenosis,* International Journal of Non-Linear Mechanics, 40(2005), 151-164.

[2] J. Enderle, B. Susan & B. Bronzino, *Introduction to Biomedical Engineering,* London: Academic Press, 2000.

[3] S.E. Charm & G.S. Kurland, *The Flow Behavior and Shear Stress, Shear Rate Characteristics of Canine Blood,* Am. Journal of Physiology, 203(1962), 417–421.

[4] K. Perktold, R. Peter & M. Resh, *Pulsatile non-Newtonian Blood Flow Simulation Through a Bifurcation with an Aneurism*, Biorheology, 26(1989), 1011-1030.

[5] M.A. Hussain, K. Subir & R.R. Puniyani, *Relationship Between Power Law Coefficients and Major Blood Constituents Affecting the Whole Blood Viscosity*, Journal of Bioscience, 24(1999), 329–337.

[6] C. Tu & M. Deville, *Pulsatile Flow of non-Newtonian fluids Through Arterial Stenoses*,Journal of Biomechanics,29(1996),899-908.

[7] N. Talukder, P.E. Karayannacos, R.M. Nerem & J.S. Vasko, *An Eperimental Study of the Fluid Dynamics of Multiple Noncritical Stenoses*, Journal of Biomechanical Engineering, (1977), 74-82.

[8] T. Fukushima, T. Azuma & T. Matsuzawa, *Numerical Analysis of Blood Flow in the Vertebral Artery,* Journal of Biomechanical Engineering, 104(1982), 143-147.

[9] P.R. Johnston, D. Kilpatrick, *Mathematical Modelling of Paired Arterial Stenoses*, Computers in Cardiology, (1990), 229-232.

[10] K.C. Ang & J. Mazumdar, *Mathematical Modeling of Triple Arterial Stenoses*, Australian Physical and Engineering Sciences in Medicine, 18(1995), 89-94.

[11] P.R. Johnston & D. Kilpatrick, *Mathematical Modelling of Flow Through an Irregular Arterial Stenosis,* Journal of Biomechanics, 24(1991), 1069-1077.

[12] H.I. Anderson, R. Halden & T. Glomsaker, *Effects of Surface Irregularities on Flow Resistance in Differently Shaped Arterial Stenoses,* Journal of Biomechanics, 33(2000), 1257-1262.

[13] S. Chakravarty, P.K. Mandal & Sarifuddin, *Effect of Surface Irregularities on Unsteady Pulsatile Flow in a Compliant Artery,* International Journal of Non-Linear Mechanics, 40(2005), 1268-1281.

[14] A. Yakhot, L. Grinberg & N. Nikitin, *Modelling Rough Stenoses by an Immersed-boundary Method*, Journal of Biomechanics, 38(2005), 1115-1127.

[15] R.B. Bird, W.E. Stewart & E.N. Lightfoot, *Transport Phenomena,* Wiley International Edition, 1960.

[16] T.J. Pedley, *The Fluid Mechanics of Large Blood Vessels,* Cambridge University Press, London, 1980.

[17] A.C. Burton, *Physiology and Biophysics of the Circulation,* Introductory Text, Year Book Medical Publisher, Chicago, (1966).

[18] L.H. Back, Y.I. Cho, D.W. Crawford & R.F. Culel, *Effect of Mild Atherosclerosis on Flow Resistance in a Coronary Artery Casting of Man,* ASME Journal of Biomechanical Engineering, 106(1984), 48-53.